Dear Prof Kantha,
Please find the revised version of the manuscript OS-12-1669 by Brando et al.

All general and specific comments by the reviewers were addressed. Please find enclosed to the letter a table with a point-to-point response to the reviewer's comments, and a track-change version of the manuscript. The manuscript has been carefully edited.

Following the reviewers comments, more details were added throughout the manuscript:

Three new paragraphs were added to the introduction:
- One to detail the Horner -Devine et al (2015) plume dynamical regions
- One to describe the main circulation patterns in NAS and the role of wind- and wave-driven resuspension on the turbidity dynamics in NAS
- One to describe the manuscript structure

A new figure (Figure 3) detailing the circulation patterns prior to and at the acquisition date of the Landsat-8 image was added with corresponding text to strengthen sections 3.1.

Figures 4 and 5 (now 5 and 6) were redrawn to improve readability.

In Sections 3.3 and 3.4 the SST and T fields were commented in relation to published literature for NAS.

Figure 5c (now Figure 7) was improved by including also SSS.

A new section was added (3.5) to describe the relations between SST, T and SSS in Figures 5,6 and 7.

In section 3.6 (previously 3.5) a paragraph was added referring to the broad classification of the plumes carried out by Syvitski et al. (2005).

During the revision of the manuscript we decided to not add another Landsat 8 image from a "normal" condition. To select a "normal condition" we briefly analyzed all L8 images of NAS, but they all show different patterns, depending on wind, wave and flow regimes. This work will be described separately in a separate manuscript. In our view, adding a new figure, as suggested by both reviewers, would entail justifying the selection of an appropriate date for the comparison and then describing all associated meteo-marine conditions. This would lengthen considerably the manuscript and change its focus.

We wish to thank reviewers for the insightful comments.
Regards,
Vittorio Brando

Reviewer 1
Specific comments

R1_S1	- It'd be interesting to show another L8 image (either RGB or T or SST) to show a "normal" or non flooded situation to highlight the difference in the properties found in the two cases.	A new figure with a new another L8image was not be added to the manuscript. In our view, adding a new figure would entail justifying the selection of an appropriate date for the comparison, describing all associated meteo-marine conditions and it would lengthen the manuscript. The results of this work were discussed in reference to published work on NAS SST and turbidity dynamics in sections 3.3 and 3.4. See also response to R2_G2
R1_S2	- Is there any reference in the literature about this near-shore trapped warm waters (NTTW)? Have they been previously described? What do the authors think or hypothesize about the origin of these waters?	We changed the acronym in the manuscript to NTWW to better reflect "near-shore trapped warm water". We are not aware of any other studies. based on remote sensing or modelling, describing similar structures in the Po Delta area or in NAS. Thus, in the first paragraph of the conclusions we added a statement "To our knowledge, this study provided the first evidence of NTWWs in NAS." As we are lacking detailed information on the vertical structure of this observed phenomenon we are not ready to speculate on the underlying processes. Hence, we added to the conclusions a recommendations for "dedicated field and numerical investigations are needed to characterize the temporal evolution of the spatial and vertical

		structure of the SSS, SST and T fields of river plumes interacting with the receiving waters and among them in varying discharge conditions. This would also enable to define the processes leading to the occurrence of NTWWs."
R1_S3	- In order to show more clearly the relation between the three variables analyzed (T, SST and SS) information of SSS for each site could be included in Figure 5c in different colors, while the shape could be used to identify their location	The figure was improved as suggested in the revised version (now figure 7). A new section (3.5) describing the dilution pathways and the relationships between SSS, SST and T was added to the manuscript
R1_S4	- In Section 3.5, it is mentioned that the two ROFIs identified are "Plume F" type, following Horner-Devine et al. (2015) classification. And it's stated that the borders can be identified by the 36 isohaline corresponding to the 5 FNU and $18 \circ$C isotherm. From figures 4 and 5 this seems to be the case for the cyclonic coastal current, but not for the western rivers, where the 36 isohaline does not correspond with the $18 \circ$C isotherm or 5 FNU isoline, but is located further offshore. Thus both SST and T seems not to be good indicators of the region of freshwater influence. Include some discussion in the text about this.	To enable a thorough description of the ROFI boundaries in section 3.4 Figure 5 b(now figure 6) was extended to show the outer boundaries of the Po river plume. In section 3.4 we clarified the use of the 3 and 5 FNU isolines to delineate the surface expression of the plumes in the T field from the adjacent ocean waters (Fig. 6). Also we added a new section (3.5) describing the dilution pathways and the relationships between SSS, SST and T, and a revised detailed text in section 3.6 (previous 3.5) addressing this comment.
R1_S5	- Using in situ data and simulations Dogliotti et al. (2015) showed that uncertainty for turbidity estimation is expected to be low (typically less than 6% using simulations and ~13% from in situ data). Thus, the high variability in the composition of the region is not expected to affect the algorithm accuracy, but the relationship between T and suspended matter	A statement on the accuracy was added to section 2.1. The statement of the future work on the conclusions was revised according to this comment: "The observed optical complexity of NAS due to the variability in composition of the particulate matter may affect accuracy of the Dogliotti et al.

	concentration for each river. Indeed, future work is needed to characterize the optical properties including side-scattering (turbidity), i.e. to validate the cited algorithm.	(2015) algorithm for T retrievals, and the relationship between T and suspended matter concentration for each river. Hence future work is needed to characterize optical properties of particulate and dissolved matter delivered by each river in flood and non-flood conditions. This will also enable the validation of the Dogliotti et al. (2015) algorithm and the parameterization of other OCR algorithms (e.g. Melin et al., 2011;Vantrepotte et al., 2012;Brando et al., 2012) to accurately retrieve chlorophyll and suspended matter concentrations in these complex coastal waters."

Technical corrections

R1_D1 Page 1672, line 22:	During this combines flood event a total of ~15 km3 of freshwater entered NAS, ~10 km3 of which entered the basin by 19 November 2014.	done
R1_D2 Page 1673, line 5:	change the future to the past tense in order to use the same tense in the whole paper, i.e. In this study we combined SST and turbidity maps derived from L8 imagery...	done
R1_D3 Page 1673, line 9:	change "plume" with "plumes' " in ... interpretation of the plumes' dynamic and their interaction...	done
R1_D4 Page 1673, line 17:	Define VNIR and SWIR acronyms	done
R1_D5	Define SNR	done

Page 1673, line 18:		
R1_D6 Page 1674, line 5:	Please, give more details regarding the atmospheric correction. Which bands were used: NIR (VR 2014) or SWIR (VR 2015)? In case of the later, epsilon was calculated on a pixel basis or it was calculated for the whole scene or a sub-scene?	As recommended in the manual of ACOLITE (v. 20150701), in the case of moderately to extremely turbid waters (turbidities > ~30 FNU), we applied the SWIR atmospheric correction (Vanhellemont and Ruddick, 2015), with a per-pixel variable aerosol epsilon. These details were added to section 2.1
R1_D7 Page 1674, line 10:	did the authors mean top-of-atmosphere brightness temperature?:	Yes, corrected
R1_D8 Page 1674, line 11	add wavelength of L8 band 10 for clarity (10.9 um)	done
R1_D9 Page 1674, line 21:	define ARPA	done
R1_D10 Page 1675, line 2:	add "the" in: ...followed by the effect of increasing...	done
R1_D11 Page 1675, line 7:	change of with than ("...smaller than 0.3 m.")	done
R1_D12 Page 1676, line 13:	associate the spectra from the center of the basin with the name given in Fig. 3. e.g. "the spectra for the center of the basin (indicated as open waters in Fig. 3a) have a peak at 443 and 482 nm, typical of blue waters..."	done

R1_D12 Page 1676, line 16:	add a comma (,) after "... a 562 nm peak, typical of green waters..."	done
R1_D13 Page 1676, line 25:	change "similarly" to "similar to values found at rho(655)"	done
R1_D14 Page 1677, line 5:	add "the" in "The yellow /brown shades of the other rivers..."	done
R1_D15 Page 1678, line 18:	Add FNU after 10-30 range	done
R1_D16 Page 1679, line 3-4:	add "than" after higher	done
R1_D16 Page 1681, line 21:	Add a comma (,) after "Moreover,"	done

Rev2

R2_G1	However, in order to make the analysis clearer, and the manuscript suitable for publications, the authors should provide a better introduction regarding what a "river plume characterization" means. This will give to the reader a better understanding of the main goal of this work and its potential.	A new paragraph was added at the end of the introduction to clarify the aims of this work.
R2_G2	The authors focus on the 19 November 2014 flood	A new figure with a new another L8image was not

	event. I believe that such an analysis needs to be complemented by a comparison with satellite, optical measurements during a steady state condition (either a climatologic pattern or a low water discharge state) in order to actually recognize the role of river outflow momentum during the flood.	be added to the manuscript. In our view, adding a new figure would entail justifying the selection of an appropriate date for the comparison, describing all associated meteo-marine conditions and it would lengthen the manuscript. Further than the particulate matter associated with freshwater discharge the turbidity dynamics of the NAS is controlled by wind and wave driven resuspension. A new paragraph was introduced in the introduction to describe these processes. The results of this work were discussed in reference to published work on NAS SST and turbidity dynamics in sections 3.3 and 3.4.

R2_S1	The authors state that they "characterize river plumes in the NAS" but it is not clear what such a characterization means until the discussions. The manuscript will be much clearer if the authors specify, from the beginning, that the goal is to provide an optical/lithological as well as spatial characterization of those plumes. For this purpose, they should briefly summarize, in Introduction, the scheme proposed by Horner-Devine et al. (2015). In this way the reader will follow the analysis and the discussions (Section 3.5, in particular) in a better way.	The scheme proposed by Horner-Devine et al. (2015) was summarized in the introduction and in the new section 3.5. We strengthened the final paragraph of the introduction to describe the aims of the this work.
R2_S2	Something missing in Introduction is a brief comment regarding other satellite sensors that are often used for coastal and river plume waters. The authors should	To clarify the transition from OCR sensor to Landsat, two new sentence were added here: "These studies were based on data acquired from

	provide a sentence that explains why the preferred the L8 with respect to other satellites (e.g., MODIS). I believe that their goal was to recognize the "fine structure" of the plumes and thus they preferred to go for a high spatial resolution approach. All this need to be stated.	MODIS, SeaWiFS or AVHRR sensors with a 1-4 km spatial resolution and 1-3 days revisit time. (Dickey et al 2003)." "Historically Landsat data has been used in coastal and inland waters to map both particulate matter and surface temperature at finer spatial resolution (~30m and ~100m respectively) (Hellweger et al., 2004;Fisher and Mustard, 2004)."
R2_S3	I would suggest to add an additional section that provides a better introduction of the NAS circulation and the role that river inputs have on it.	In the introduction we expanded the description of NAS providing more details on the general circulation, detailing the effects of winds and river discharge.
R2_S4	The analysis does not include any in situ data for calibration and validation of the satellite measurements. A comment on this (in the methodologies) would be appreciated.	A statement on the accuracy was added to section 2.1. Please see also response to R1_S5
R2_S5	It is not clear to me what the SSS (provided by the numerical model) adds. I see two main issues here: i) spatial resolution of the model is much lower than the satellite one; ii) while for the Po River input the numerical simulation considers the actual (daily or hourly) water discharge, for the other rivers the authors consider monthly climatological estimates (Page 1674; Line 28). Both issues weaken some of the discussions in Section 3.3. My suggestion is to restrict the SSS analysis to the Po River plume only, where the SSS and SST fields are more coherent and allow for a better discussion.	We feel that showing that current resolution and that the (lack of) available near real-time inputs of the operational model have some limits in describing such an extreme event may be useful for the local scientific community. Hence, in section 3.3 we clarified that the mesoscale patterns are well captured, while difference arise at submesocale and fine scale due to differences in resolution and the lack of near real-time data for freshwater discharge. Also in the revised version we strengthened section 3.1 by adding a new figure describing the modeled circulation patterns.

| R2_S6 | As I mentioned in the general comment, I was expecting to see a comparison between the river plume patterns during a high water discharge event and a low stage state. In this way, the authors can really quantify the role of riverine outflows in forming the bulges and delivering sediments. | Please, see response to R2_G2 |

Minor Comments

R2_D1 Page (167)1, Line 5:	I would not write that the SSS field "support" the interpretation but rather may add some additional information (for the Po River plume only, see Specific comments).	As we are now also using the model outputs to describe the circulation patterns, we believe that it is appropriate to use the term "support"
R2_D2 Line 20:	Rephrase as "by advection and mixing processes".	Done
R2_D3 Line 23:	I think the authors should include those two references: Geyer et al. [Continental Shelf Research 24 (2004) 927–949], Nof and Pichevin [Journal of Physical oceanography 31 (2001), 3045-3058].	Done, thanks for the suggestion
R2_D4 Line 23-24:	Rephrase as "importance of these processes".	done
R2_D5 Page 2, Line 13:	add Bignami et al. [Journal of Geophysical Research: Oceans 112 (2007) 1978–2012].	Done, thanks for the suggestion.
R2_D6 Line 27:	same as Line 13.	Done
R2_D7	I think, before this paragraph, authors should provide a	Please see response to R2_S2

Page 3, Line 3:	comment regarding other satellites that are often used for coastal and river plume waters (e.g., MODIS) as well as a sentence that explains why the preferred the L8 with respect to other satellites (see specific comments).	
R2_D8 Line 8-10:	As I mentioned I do not believe that the COAWST model "support" the interpretation, but rather it may add some additional information (this is true for the Po River mouths only; see specific comments). Please, rephrase this sentence.	Please see response to R2_D1
R2_D9 Line 10:	Please, indicate here the spatial resolution of the model.	To simplify the sentence, the resolution of the satellite was removed
R2_D10 Page 5, Line 19:	a dedicated section on the general circulation of the NAS will make this sentence more robust.	Done, please see response to R2_S3
R2_D11 Page 5, Line 24-	Where are these data from? Please, specify	This data were from the model outputs. We strengthened section 3.1 by referring to a new figure (Fig 3) describing the modeled circulation patterns.
R2_D12 . Page 6, Line 13:	I would rephrase as "the spectra for the offshore part of the basin".	done
R2_D13 Page 7, Line 1-13:	Maybe I am wrong, but I believe that all this part would be much more quantitative if the authors provide a plot for the ratios 865/655 and 655/562 (and a consequent discussions based on it.	We tried to plot the suggested ratios but we found the figure very difficult to interpret and describe. Hence we will not include this plot in the revised version.
R2_D14 Line 5:	isn't it this true for the Brenta, Livenza, and Sile too?	Two sentences were added to section 3.2, one for the Brenta river an one for the rivers draining the floodplain and agricultural soils

R2_D15 Figure 3:	The plot legend is in common for the two panels. I would suggest moving it in the middle of them.	The proposed change was not be implemented.
R2_D16 Figure 4:	The colorbar is missing here. Moreover, I would suggest including a metric scale (as the authors did for Figure 1). Finally, there is an error on the isohaline 37 (which is marked as 36).	The figure was redrawn.

High resolution satellite turbidity and sea surface temperature observations of river plume interactions during a significant flood event

V. E. Brando[1,2], F. Braga[3], L. Zaggia[3], C. Giardino[1], M. Bresciani[1], E. Matta[1], D. Bellafiore[3], C. Ferrarin[3], F. Maicu[3], A. Benetazzo[3], D. Bonaldo[3], F. M. Falcieri[3], A. Coluccelli[4], A. Russo[4,5], S. Carniel[3]

[1] {Consiglio Nazionale delle Ricerche – Istituto per il Rilevamento Elettromagnetico Ambientale (CNR-IREA), Via Bassini 13, 20133 Milano, Italy}

[2] {Commonwealth Scientific & Industrial Research Organization (CSIRO), Canberra, Australia}

[3] {Consiglio Nazionale delle Ricerche – Istituto di Scienze Marine (CNR–ISMAR), Arsenale-Tesa 104, Castello 2737/F, 30122 Venezia, Italy}

[4] {Università Politecnica delle Marche – Dipartimento di Scienze della Vita e dell'Ambiente (UNIVPM-DISVA), Via Brecce Bianche, 60131 Ancona, Italy}

[5] {NATO STO Centre for Maritime Research and Technology, V.le San Bartolomeo 400, 19126 La Spezia}

Correspondence to: V. E. Brando (brando.v@irea.cnr.it)

Abstract

Sea surface temperature (SST) and turbidity (T) derived from Landsat-8 (L8) imagery were used to characterize river plumes in the Northern Adriatic Sea (NAS) during a significant flood event in November 2014. Circulation patterns and sea surface salinity (SSS) from an operational coupled ocean-wave model supported the interpretation of the plumes interaction with the receiving waters and among them.

There was a good agreement of the SSS, T, and SST fields at the sub-mesoscale and mesoscale delineation of the major river plumes. L8 30m resolution enabled also the description of smaller plume structures. The different plumes reflectance spectra were related to the lithological fingerprint of the sediments in the river catchments.

Sharp fronts in T and SST delimited each single river plume. The isotherms and turbidity isolines coupling varied among the plumes due to differences in particle loads and surface temperatures in the discharged waters. The surface expressions of all the river plumes

occurring in NAS were classified based on the occurrence of the plume dynamical regions in the L8 30 m resolution imagery.

1   Introduction

Riverine discharges in the coastal ocean form river plumes, distinct regions where water masses properties are significantly influenced by riverine freshwater as it merges into ocean waters with different thermohaline and dynamical properties (Horner-Devine et al., 2015). The extent, motion, and general structure of river plumes are mainly determined by the advection and mixing processes of freshwater from the river mouth, while the along-coast transport of the river-borne material is determined by several processes, including stratified-shear mixing, frontal processes, oceanic transport, tide and wind forcing, as well as Coriolis effects (Hetland, 2005;Horner-Devine et al., 2015;Geyer et al., 2004;Nof and Pichevin, 2001). The relative importance of these processes determines the overall fate and transport of freshwater, as well as the associated dissolved and particulate matter within the plume (Horner-Devine et al., 2015;Devlin and Schaeffelke, 2009;Brodie et al., 2010;Syvitski et al., 2005).

Following Horner-Devine et al. (2015, and references therein), the river plume structures can be described in terms of four regions characterized by different dominant dynamical balances: 1) the source region, where the buoyancy and momentum that initiate a river plume are determined by estuarine processes; 2) a jet-like near-field region of initial plume expansion; 3) an unsteady, anticyclonic eddy circulation, i.e. a "bulge", that accumulates a fraction of the river discharge; and 4) a region beyond where the plume water has lost all memory of the inflow momentum but is still distinct from the ambient receiving water, i.e. a far-field plume or coastal current.

Within the Mediterranean Sea, the Northern Adriatic Sea (NAS, Fig. 1) is the sub-basin most influenced by river plumes (DeGobbis et al., 2000;Spillman et al., 2007;Falcieri et al., 2014). The NAS is a shallow (average depth is smaller than 35 m) and semi-enclosed regional sea, which due to the high amount of freshwater is generally considered a dilution basin (DeGobbis et al., 2000;Spillman et al., 2007). Riverine input along the Northern Adriatic coast is generally associated to sharp coastal fronts and significantly contributes in driving a southeastward current along the Italian coast (Bergamasco et al., 1999), while mechanisms and sub-mesoscale patterns of plume spreading within the basin are strongly controlled by the

modulation of freshwater discharge and wind regime (Bignami et al., 2007;Falcieri et al., 2014;Spillman et al., 2007;Tesi et al., 2011). Sediment dispersal in the basin is mostly controlled by the wave action generated by dominant and prevailing winds blowing on the Adriatic Sea: (namely, Bora and Sirocco; e.g. Sclavo et al., 2013;Boldrin et al., 2009).

During flood events the Po, Adige and Brenta rivers produce an almost single river plume, contributing 84% of the total freshwater discharge delivered to the basin (Cozzi and Giani, 2011;Falcieri et al., 2014). However, the local effects of the northern rivers (form Isonzo to Piave rivers, Fig. 1) is considerable, since they can contribute with low-salinity patches that are relevant to mesoscale and sub-mesoscale dynamics (Marini et al., 2008;Solidoro et al., 2009). These freshwater discharges and associated particulate and dissolved matter inputs have a significant effect both on the physical and biogeochemical properties of the whole basin (Zavatarelli et al., 1998;Marini et al., 2008;Solidoro et al., 2009;Bignami et al., 2007;Barale et al., 1986;Tesi et al., 2011)

Following a large regional precipitation event affecting northern Italy, in November 2014 all NAS rivers flooded concurrently (Fig. 2). Peak discharge for the Po River reached 8375 m^3s^{-1} on 19 November 2014, the fifth highest of the last hundred years (Montanari, 2012). The timing of the flood for each river varied reflecting the space-time distribution of precipitation and catchment morphology: Piave, Brenta and Isonzo peaked earlier on 6-7 November, Livenza and Adige on 8 November, while Po peaked the first time on 9 November (~4000 m^3s^{-1}) and then reached the maximum discharge on 19 November. During this combined flood event a total of ~15 km^3 of freshwater entered NAS, of which ~10 km^3 entered the basin by 19 November 2014, equating to ~1% of the basin volume.

Earth observation has been widely used to describe mesoscale dynamics and physical oceanographic characteristics of river plumes fronts using sea surface temperature (SST) and ocean colour radiometry (OCR) sensors (e.g. Ullman and Cornillon, 1999;D'Sa et al., 2007;Palacios et al., 2009;Schroeder et al., 2012;Brodie et al., 2010). Several studies have combined SST with OCR data and/or with model data to quantify the extent, strength and variability of the river plumes fronts and to explain their behaviour in relation to the main physical forcing processes (e.g. Hickey et al., 2005;Otero et al., 2009;Pietrzak et al., 2011;Falcini et al., 2012;Margvelashvili et al., 2013;Bignami et al., 2007). Most of these studies were based on data acquired from MODIS, SeaWiFS or AVHRR sensors with a 1-4 km spatial resolution and 1-3 days revisit time (Robinson, 2010).

Historically Landsat data has been used in coastal and inland waters to map both particulate matter and surface temperature at finer spatial resolution (~30 m and ~100 m respectively) (Hellweger et al., 2004;Fisher and Mustard, 2004, and references therein). The recently launched Landsat-8 (L8) has been deemed suitable for studying aquatic environments due to improved data quality and spectral coverage (Irons et al., 2012;Pahlevan et al., 2014).

In this study we combined SST and turbidity (T) derived from L8 imagery to describe at fine spatial resolution river plumes and their sub-mesoscale interactions in the NAS during the significant combined flood event of November 2014. To this aim we used the model data from an operational coupled ocean-wave modelling system to support the interpretation of the plumes' dynamics and their interaction with the receiving waters and among them. Section 2 provides details on the satellite imagery processing and on the operational coupled ocean-wave modelling system, while in section 3 the optical and spatial characterization of the river plumes based on T and the SST fields is presented. In this work we classified the surface expressions of all the river plumes occurring in NAS based on L8 30 m resolution imagery following the Horner-Devine et al. (2015) classification scheme for plume morphology, thus extending the broad classification carried out by Syvitski et al. (2005) using MODIS imagery at 250 m resolution.

2 Methods

2.1 Satellite imagery

To image the Earth throughout the visible and thermal portions of the spectrum, L8 carries two separate sensors, the Operational Land Imager (OLI) and the Thermal Infrared Radiometer Sensor (TIRS). Both OLI and TIRS represent an evolution in Landsat sensor technology in terms of data quality and spectral coverage (Irons et al., 2012). The OLI provides coverage of the visible, near infrared and shortwave infrared (SWIR) portions of the spectrum at 30 m spatial resolution in nine spectral bands with a relatively high signal to noise ratio (~300 for the blue bands) (Irons et al., 2012;Pahlevan et al., 2014). OLI data is considered particularly adequate for ocean colour retrievals and turbidity mapping due to its radiometric resolution and calibration accuracy (Pahlevan et al., 2014;Vanhellemont and Ruddick, 2014;Franz et al., 2015). The TIRS adds two long-wave thermal spectral bands at 100 m spatial resolution, centred at 10.9 and 12.0 μm (bands 10 and 11, respectively) (Irons et al., 2012). As these two Landsat 8 datasets are complementary, they are distributed as combined data products, where the TIRS 100 m pixels are resampled and co-aligned with the

OLI 30 m data (Irons et al., 2012;Storey et al., 2014).

In this study we used OLI and TIRS imagery of 19 November 2014 capturing a significant freshwater inflow into the NAS for mapping both T and SST. For turbidity, OLI data were converted into water-leaving radiance reflectance (ρ_w, dimensionless) with ACOLITE, an automatic method for atmospheric correction designed specifically for OLI over turbid waters (Vanhellemont and Ruddick, 2014, 2015). As recommended in moderately to extremely turbid waters (Vanhellemont and Ruddick, 2015), a per-pixel variable aerosol type was determined from the ratio of reflectances in the SWIR bands (1609, 2201 nm), after having applied the Pahlevan et al. (2014) radiance gains for radiometric calibration. The ρ_w data were then converted into T expressed in Formazin Nephelometric Unit (FNU) following Dogliotti et al. (2015). As at higher T values, ρ_w (655nm) starts to saturate while ρ_w (865nm) still linearly increases with T, they use a switching scheme to avoid saturation at 655 nm and retrieve accurately T in the 1-1500 FNU range (within ~13% of in situ data, Dogliotti et al., 2015). SST values were retrieved from top-of-atmosphere brightness temperature in TIRS band 10 (10.9 μm) with a radiative-transfer based atmospheric correction (Barsi et al., 2014;Barsi et al., 2005).

2.2 Hydrodynamic forecasting model

As a complement to the L8 images, we analysed model data generated by an operational implementation in the northern Adriatic basin of the Coupled Ocean-Atmosphere-Wave-Sediment Transport (COAWST,Warner et al., 2008) where the Regional Ocean Modeling System (ROMS) and the Simulating Wave Nearshore (SWAN) model are 2-way fully coupled (Russo et al., 2013b;Russo et al., 2013a). COAWST was implemented for the NAS on a grid with horizontal spacing of 0.5 km and 12 vertical terrain-following *s*-levels, offline nested to parent operational models covering the whole Adriatic and the Italian seas (Russo et al., 2013b;Russo et al., 2013a). The operational systems were forced by the operational high-resolution (7 km x 7 km) meteorological model COSMO-I7 (Russo et al., 2013b;Russo et al., 2013a). Following Hetland (2005), at the river mouths grid cells momentum was injected giving a vertical structure to the plume, i.e. injecting most of the freshwater discharge in the surface layers (~ 80% in the four uppermost sigma levels, corresponding to about 1.5 m). Daily time series of freshwater supplies from the Po river were imposed (and kept constant along the 72h of forecast), while the remaining NAS rivers were prescribed based on monthly climatological estimates (Raicich, 1994). To represent the Po river delta system, the flow measured at Pontelagoscuro (90 km upstream the river mouth) is split into five major

---

Vittorio Brando 29/9/15 2:24 PM
Deleted: turbidity

Vittorio Brando 29/9/15 2:24 PM
Deleted: turbidity (

Vittorio Brando 29/9/15 2:24 PM
Deleted:)

Vittorio Brando 29/9/15 2:24 PM
Deleted: turbidity

Vittorio Brando 29/9/15 2:25 PM
Deleted: turbidity

Vittorio Brando 29/9/15 2:25 PM
Deleted: turbidity

Vittorio Brando 30/9/15 12:20 PM
Deleted:

Vittorio Brando 13/10/15 2:18 PM
Deleted: *data*

Vittorio Brando 13/10/15 11:22 AM
Deleted: ran by ARPA Emilia Romagna)

Vittorio Brando 13/10/15 11:22 AM
Deleted: is

Vittorio Brando 15/10/15 11:18 AM
Deleted: Hetland et al.

Vittorio Brando 6/10/15 3:22 PM
Deleted: In order t

Vittorio Brando 13/10/15 11:26 AM
Deleted: out

Vittorio Brando 15/10/15 11:46 AM
Deleted: 5

branches (Maistra, Pila, Tolle, Gnocca and Goro) following the partitioning proposed in Zasso and Settin (2012). Minor Po river branches, north of the Po di Pila mouth, and some minor freshwater inputs (e.g. nearby the Caorle and Baseleghe wetlands) are not considered.

To delineate the surface extent of river plumes and the freshwater influence in the basin, the daily averaged surface level of the modelled salinity field was considered as the sea surface salinity (SSS) field. This approach explicitly does not consider the vertical structure of the plume or the mixed layer depth (as proposed in Otero et al., 2008, 2009) as the shallow waters of NAS and the weak tidal dynamics not always allow the development or the identification of a mixed layer (Falcieri et al., 2014). Hence, following Falcieri et al. (2014), in this study the surface extent of the freshwater influence in the NAS was identified with the 36 isohaline resulting from the salinity fields obtained by the numerical model.

3   Results and Discussion

In the pseudo-true colour composite of the OLI imagery of 19 November 2014 (Fig. 1) two very large regions of freshwater influence (ROFI, *sensu* Simpson, 1997) are delineated in the NAS by the convolution of the plumes generated by the northern rivers from the Isonzo to the Piave and then by the western rivers i.e., the Brenta, Adige and Po. As the river mouths are close to each other, sharp fronts delineate the river plumes from the cyclonic coastal current transporting dissolved and particulate matter from upstream plumes. The area in front of the Venice Lagoon shows specific patterns generated by the interaction between the coastal current and local tidal dynamics at the lagoon inlets, enhanced by the presence of long artificial jetties (Bellafiore, 2010).

3.1   *Meteo-oceanographic conditions*

The basin was characterized by relatively calm conditions in the days before the L8 image retrieval. Modelled regional circulation patterns in the week from 12 to 19 November 2014 were initially dominated by a southeastward current along the Italian coast (daily-average speed up to 0.7 m s^{-1} at the sea surface), although the freshwater injected in the previous days (6-11 November 2014, see Fig. 2) was already spread over a large fraction of NAS (Fig. 3a). The increasing riverine inflow progressively enhanced the effect of Po River in controlling surface circulation in the NAS, with a plume spreading offshore with strong vertical gradients in temperature and salinity (Fig. 3b). These patterns are consistent with the conditions recorded at the Acqua Alta Oceanographic Tower (AAOT) located about 15 km off the Venice Lagoon (Fig. 1), where on 19 November 2014 the average wind speed was 4 m s^{-1} and

the sea state was characterized by a mean significant wave height smaller than 0.3 m. Depth-averaged oceanic currents were weak (reaching a modelled value of 0.1 m s^{-1},) and mostly directed southwestwardly, while surface currents appeared dominated by riverine inflow. In particular, modelled surface current velocities exceeded 0.5 m s^{-1} in large coastal areas off the Po river mouths, while the propagation of the plume (isohaline 36) was characterised by velocities of approximately 0.35 m s^{-1} in large sectors of the frontal region (Fig. 3b).

3.2 Spectral properties

From a qualitative point of view, the plumes and the coastal waters in the NAS appear very different in colour ranging from white to yellow/brown shades in the pseudo-true colour composite (Fig. 1). Fig. 4 presents reflectance spectra extracted from selected locations of interest in NAS: the spectra for the center of the basin (indicated as "open waters" in Fig. 4a) have a peak at 443 and 482 nm typical of blue waters (ρ_w (482) ranging 0.01-0.03), while the AAOT, the Venice lagoon inlets (Chioggia, Malamocco and Lido) and Grado inlet of the Marano lagoon have a 562 nm peak, typical of green waters (ρ_w (562) ranging 0.04-0.07). The waters flowing from the western Marano lagoon (Lignano inlet) and Caorle and Baseleghe wetlands have higher spectra and ρ_w values at 562 and 655 nm are very similar (ranging 0.10-0.12 and 0.08-0.12, respectively).

The river plumes spectra show a peak at 655nm of whitish/yellow/brown waters (ρ_w (655) ranging 0.09-0.23, Fig. 4b). In particular, the Isonzo, Tagliamento and Piave river plumes appear as almost white in the true-colour as they have high ρ_w at both 562 and 655 nm, while the Po, Brenta, Adige, Sile and Livenza river plumes appear in yellow/brown shades, as ρ_w (562) is lower, ranging 0.08-0.12. The Po river plumes show ρ_w (865) ranging 0.10-0.12, similar to values found for ρ_w (655), whilst for all other river plume spectra ρ_w (865) was lower than the ρ_w (655).

The very high reflectances and the colours of eastern Alpine rivers (Isonzo, Tagliamento and Piave) plumes are related to carbonate-rich sediments, yielded by their prevailing Mesozoic limestone and dolomite catchments (Pigorini, 1968;Castellarin and Vai, 1982). The yellow/brown shades of all the other rivers are due to the lithological fingerprint of their sediments. The Brenta River drains a mix of carbonate, volcanic and metamorphic terrains in North-eastern Alps (Dinelli and Lucchini, 1999). The Adige River drains a metamorphic and porphyric catchment in North-eastern Alps (Dinelli and Lucchini, 1999). The Po River drains both the Alps and Northern Apennines, respectively characterized by metamorphic-intrusive

rocks and terrigenous sequence (shales, calcareous, mudstones and sandstones) (Dinelli and Lucchini, 1999). Some of the major rivers (e.g. Brenta and Po) also drain mixed river deposits of the floodplain and agricultural soil, while the remaining minor rivers, including Venice and Marano lagoons tributaries, mostly drain these reworked terrains (Piovan et al., 2010). A considerable fraction of the flux from wetland-lagoon systems, constituted by organic particulate and high dissolved matter, also contribute to the dark-brown colour.

3.3 SST and SSS fields

Following Falcieri et al. (2014), we can identify the surface extent of the freshwater influence in the NAS with the 36 isohaline resulting from the salinity fields obtained by the numerical model (Fig. 5). The freshwater discharged during the combined flood event extended 12-15 km offshore for the plumes generated by the northern rivers, ~50 km in front of the Adige and Brenta rivers and more than 60 km in front of the Po River, consistently with the Falcieri et al. (2014) high discharge plume patterns. For the northern rivers and the Po River the 35 and 36 isolines were within 2-3 km, whilst for the area in front of the Venice Lagoon and the Adige and Brenta rivers these isohalines were 20-40 km apart.

Overall, the waters delineated by the 36 isohaline were colder (~12-17 °C) than the adjacent ocean waters (SST > ~18 °C). In particular, SST ranged between 12 °C and 15 °C for the river and lagoon plumes, and between 15°C and 17 °C in the coastal current connecting the river plumes. The area in front of the Venice Lagoon was warmer than the neighbouring ROFIs (SST = 16-18 °C). The SST field was consistent with the autumn/winter flood conditions described in previous studies on the SST dynamics in NAS (Gacic et al., 1997;Barale et al., 2004;Borzelli, 2008;Bignami et al., 2007).

The over-imposed isohalines showed a good correspondence with the observed SST field in delineating at the mesoscale the major river plumes (Isonzo Tagliamento, Brenta, Adige and Po rivers). For the northern rivers between the Isonzo and the Piave, the 36 isohaline coincided with 17.5 °C isotherm, while in front of the Brenta, Adige and Po rivers the 36 isohaline coincided with the 19.5 °C isotherm. Due to the lack of near real-time data for freshwater discharge for all rivers except the Po, and as some minor freshwater inputs (e.g. the Caorle and Baseleghe wetlands) are not considered in the model, there were some areas of mismatch between the SST and SSS fields at the submesoscale, particularly in the coastal region east of the Venice Lagoon.

As the L8 TIRS 100 m pixels are resampled and co-aligned with the OLI 30 m data, the SST

data used in this study has a spatial resolution one or two order of magnitude finer than the satellite data used for previous SST studies (Gacic et al., 1997;Barale et al., 2004;Borzelli, 2008;Bignami et al., 2007). Therefore, in the L8 SST field is possible to identify small near-shore trapped warm water (NTWW) parcels, which are warmer than the adjacent plumes and the coastal current, with values similar to those of the central part of the basin (SST ranging 17-19 °C). These NTWWs are located outside of the Marano lagoon (45.71 °N, 13.23 °E), between the Sile and Piave river plumes (45.49° N, 12.64° E) and to the south of the Po di Pila (44.88 °N, 12.49 °E). These features were also spectrally different than the neighbouring waters, showing a peak typical of green waters with ρ_w (562) ranging 0.09-0.12 (Fig. 4). The occurrence and locations of these small features were not adequately captured by the model derived SSS, most likely due to resolution limits.

3.4 Turbidity field

Fig. 6 presents the maps of T for the northern rivers (Fig. 6A) and the Brenta, Adige, and Po river plumes (Fig. 6B). Close to the river mouths, the Tagliamento river plume presented the most turbid waters (T>1700 FNU), while T ranged 600-800 FNU for the Po river plumes and 100-300 FNU for the other rivers. In the cyclonic coastal gyre connecting the plumes T ranged 10-30 FNU, while for the open waters outside the ROFIs it ranged 1-5 FNU. The NTWWs were clearly identifiable also in the T field: T ranged 10-50 FNU, up to one order of magnitude lower than the neighbouring plumes and significantly higher than the open ocean waters.

As the wind and wave re-suspension was negligible during this event, T is mostly related to the suspended particle load transported by the plumes in the basin (Sclavo et al., 2013;Tesi et al., 2011;Boldrin et al., 2009). Since T higher than ~3-5 FNU can be deemed as indicative of terrestrial discharge in NAS (Boldrin et al., 2005;Boldrin et al., 2009;Tesi et al., 2011;Braga et al., 2013), these values were used to delineate the surface expression of the plumes in the T field from the adjacent ocean waters (Fig. 6). Based on the 3 and 5 FNU isolines, in this event the combined plumes of suspended matter delivered by northern rivers extended 15-18 km offshore, the plumes of Adige and Brenta rivers spread 20-28 km from the coast, while the Po River plume reached a distance of 30-50 km.

At the submesoscale, the L8-derived T field (Fig. 6) is coherent with the overall pattern of suspended matter described in previous studies based on satellite data and during autumn/winter floods, although their investigations were performed using different satellite-

derived products. For instance, Barale et al. (1984) presented the vertical attenuation coefficient variability, Bignami et al. (2007) used both the vertical attenuation coefficient and an index for turbid (Case 2) waters occurrence, while other studies (Barale et al., 1986;Bohm et al., 2003;Barale et al., 2005;Spillman et al., 2007) used OCR derived chlorophyll concentration as a proxy to describe the basin response to freshwater discharge and wind events.

3.5 Dilution pathways

Following Horner-Devine et al. (2015, and references therein), the river plume structures can be described in terms of four dynamical regions characterized by different dominant dynamical balances: 1) the source region; 2) the jet-like near-field region; 3) the "bulge" that accumulates a fraction of the river discharge; and 4) the far-field plume or coastal current. The pathway to dilution for terrestrially derived freshwater is defined by the mixing and transport processes occurring in the plumes, as the discharge salinity increases through the plume dynamical regions before its ultimate dissolution into the adjacent ocean waters (Horner-Devine et al., 2015). The sharp fronts delimiting each single river plume observed in Fig. 1, 5 and 6 appear delineated both by T and SST even if the isotherms and turbidity isolines coupling varied among the plumes due to differences in particle loads and surface temperatures in the discharged waters (Fig. 7).

Close to the river mouths (SSS < 20), the Tagliamento and Po river plumes differed both in T and SST (~12.5 °C, ~1700 FNU and ~15.5 °C, 600-800 FNU respectively, Fig. 7). The dilution of the terrestrial discharge for the Po and Tagliamento rivers towards "clear" ocean waters (i.e. T < 3 FNU, SSS > 36) consistently maintained a ~2.5 °C difference. Moreover, the T and SST coupling at the river mouth (i.e. in the near-field region) does not necessarily reflect the composition of the transported particulate matter, as the Adige and Isonzo rivers (~13 °C, ~100 FNU) or the Livenza and Brenta rivers (~14.5 °C, ~150 FNU) have similar coupling but transport different material sources as described in section 3.3.

The offshore borders of the far-field plume connecting the individual plumes - identified by the 35 and 36 isohaline - corresponded to different turbidity isolines and isotherms (Fig. 5, 6 and 7). For the northern rivers, the 36 isohaline corresponded to the 3 FNU isoline and the 17.5 °C isotherm. For the western far-field plume, the 36 isohaline was at ~60 km offshore and corresponded to the 19.5 °C isotherm and the 1-2 FNU isolines, while the 3 FNU isoline was 15 km closer to the river mouth. This pattern may be a consequence of freshwater

dilution and particles settling in the frontal region.

3.6 Plume morphologies

Based on the presence/absence of the four dynamical regions, Horner-Devine et al. (2015) proposed a classification of six plumes morphologies (plumes A-F). The surface expressions of these morphologies can be identified in Fig. 1, 5 and 6 for the NAS plumes observed on 19 November 2014:

- The Isonzo, Tagliamento, Piave, Adige and Brenta rivers form "prototypical" plumes ("plume A"), comprising all dynamical regions: the initial jet-like plume expansion forms a bulge that then merges in the coastal current.

- The Livenza River jet-like plume merges in the coastal current without forming an anticyclonic eddy, probably because of the very long jetties, hence it may be classified as non rotational plume ("Plume B").

- The freshwater discharged in the western side of the Marano Lagoon forms on the sea-side a wide estuary plumes type ("plume C"). In this case the tidal dynamics lead to have no clear near-field, a weak mid-field, and no bulge.

- The discharge from the Baseleghe wetland forms an "angled inflow" plume ("plume D"), showing no bulge, due to a significant component of alongshore momentum as the inflow is at a small angle to the coast.

- The Po River enters the NAS through a deltaic system, delivering freshwater via five main river channels. The Po River Delta plume is thus the "convolution" of multiple plumes formed by each of the 12 channel outlets interacting with each other ("plume E"). Plume dynamics for each single plume depends of the river flow thrust in the branch and on behaviour of neighbouring plumes. The plumes at the mouth of the various branches carry similar concentration of particulate matter (T=600-800 FNU, Fig. 6 and 7), even if they differ in proportion of freshwater discharge and ability to transport sediment away from the coast.

- The shallow characteristics of the whole NAS littoral zone allow the identification of wider coastal areas where several rivers contribute to a common hydrological and hydrodynamic pattern. The interactions of the northern rivers plumes from the Isonzo to the Piave River and then of the western rivers - the Brenta, Adige and Po river plumes - form two distinct ROFIs ("Plume F") where the plume water has lost

memory of the inflow momentum but is still distinct from the ambient receiving water. The offshore borders of these ROFIs corresponded to different turbidity isolines and isotherms: the 36 isohaline corresponded to the 3 FNU isoline and the 17.5 °C isotherm for the northern ROFI, and to the 19.5 °C isotherm and 1-2 FNUs for the western ROFI.

- The Venice Lagoon, as a specific transitional water body with scarce freshwater sources in its interiors, could not properly be classified as a ROFI. Coastal circulation in front of the lagoon is dominated by tidal dynamics and the presence of jetties and breakwaters at the inlets is highly influencing the shaping of less salty water (but still not freshwater) tidal plumes (Bellafiore, 2010).

The classification of the surface expressions of all the river plumes occurring in NAS based on L8 30 m resolution imagery extends the broad classification carried out by Syvitski et al. (2005) for the combined NAS rivers flood of December 2000 using MODIS imagery at 250m resolution, where the northern rivers generated "jet-like plumes", while the Po River delta produced a "more diffusive plume".

4   Conclusions

In this study, the combined use of high-resolution OCR and SST imagery enabled the identification of the dynamical regions at small scale and sub-mesoscale for all plume structures and their interactions in the NAS. The independent satellite observations of T and SST were used as tracers for the surface expression of the freshwater influence in this significant flood event. This was corroborated by the good agreement of the patterns in these fields with the modelled SSS field at the sub-mesoscale and mesoscale. Furthermore, the radiometric and spatial resolution of the L8 OLI and TIRS imagery enabled the classification of the NAS plumes of 19 November 2014 based on their morphology including the description of smaller plume structures and the NTWWs, whilst these features were not adequately resolved by the 500m resolution of the SSS model data. To our knowledge, this study provided the first evidence of NTWWs in NAS.

Although the event discussed in this study was captured with a sensor having a revisiting time of 16 days, we expect that with the recent launch of ESA's Sentinel 2A and the forthcoming launch of Sentinel 2B the temporal resolution will increase reaching almost those normally associated with OCR missions (Dickey, 2003;Hestir et al., 2015;Mouw et al., 2015). Combined with their radiometric resolution similar to OCR missions, these

developments will thus offer an opportunity to also describe the temporal evolution of plume structures at the sub-mesoscale.

The observed optical complexity of NAS due to the variability in composition of the particulate matter may affect accuracy of the Dogliotti et al. (2015) algorithm for T retrievals, and the relationship between T and suspended matter concentration for each river. Hence future work is needed to characterize the inherent and apparent optical properties of particulate and dissolved matter delivered by each river in flood and non-flood conditions. This will also enable the validation of the Dogliotti et al. (2015) algorithm and the parameterization of other OCR algorithms (e.g. Melin et al., 2011;Vantrepotte et al., 2012;Brando et al., 2012) to accurately retrieve chlorophyll and suspended matter concentrations in these complex coastal waters.

There are almost no studies on the partitioning of water and sediment fluxes through distributary branches of a delta or adjacent rivers due to the complexity and cost associated with a simultaneous sampling effort at all branches or rivers (Syvitski et al., 2005). Moreover, flood events are difficult to observe *in situ*, as with ship-based activities is seldom possible to reach river mouths while autonomous vehicles are not operating in shallow waters or in high-density gradients (Hetland, 2005;Devlin and Schaeffelke, 2009;Tesi et al., 2011). On the other hand, observations from instrumented sites or coastal observatories such as AAOT provide detailed information on a large array of variables but do not provide a sufficient spatial coverage and may happen not be located favourably to observe events of interest (Dickey, 2003). Hence, dedicated field and numerical investigations are needed to characterize the temporal evolution of the spatial and vertical structure of the SSS, SST and T fields of river plumes interacting with the receiving waters and among them in varying discharge conditions. This would also enable to define the processes leading to the occurrence of NTWWs.

The potential of an integrated use of earth observation, numerical models, and *in situ* observations for describing coastal dynamics has been progressively emphasized in recent years (e.g. Dickey, 2003;Staneva et al., 2009;Stanev et al., 2011). The adoption of triple-collocation algorithms will allow the intercalibration of quantities and properties retrieved from the different sources (Janssen et al., 2007 and references therein). Furthermore, the use of the independent data sets will enable the identification of the relevant time- and space-scales for the observed (and modelled) phenomena (Chang et al., 2002).

Acknowledgements

Vittorio Brando 30/9/15 2:21 PM
Deleted: e

Vittorio Brando 15/10/15 11:57 AM
Deleted: CNR

References

Barale, V., Rizzoli, P. M., and Hendershott, M. C.: Remotely Sensing the Surface Dynamics of the Adriatic Sea, Deep-Sea Res, 31, 1433-1459, Doi 10.1016/0198-0149(84)90081-5, 1984.

Barale, V., Mcclain, C. R., and Malanotterizzoli, P.: Space and Time Variability of the Surface Color Field in the Northern Adriatic Sea, J Geophys Res-Oceans, 91, 2957-&, Doi 10.1029/Jc091ic11p12957, 1986.

Barale, V., Schiller, C., Villacastin, C., and Tacchi, R.: The Adriatic Sea surface temperature historical record from Advanced Very High Resolution Radiometer data (1981-1999), Int J Remote Sens, 25, 1363-1369, 10.1080/01431160310001592300, 2004.

Barale, V., Schiller, C., Tacchi, R., and Marechal, C.: Trends and interactions of physical and bio-geo-chemical features in the Adriatic Sea as derived from satellite observations, Sci Total Environ, 353, 68-81, 10.1016/j.scitotenv.2005.09.060, 2005.

Barsi, J. A., Schott, J. R., Palluconi, F. D., and Hook, S. J.: Validation of a Web-Based Atmospheric Correction Tool for Single Thermal Band Instruments. , Earth Observing Systems X, San Diego, CA., August 2005, 2005.

Barsi, J. A., Schott, J. R., Hook, S. J., Raqueno, N. G., Markham, B. L., and Radocinski, R. G.: Landsat-8 Thermal Infrared Sensor (TIRS) Vicarious Radiometric Calibration, Remote Sens., 6, 11607-11626, , doi:10.3390/rs61111607., 2014.

Bellafiore, D., and G. Umgiesser: Hydrodynamic coastal processes in the North Adriatic investigated with a 3D finite element mode, Ocean Dynam., 60, 255-273, doi:10.1007/s10236-009-0254-x., 2010.

Bergamasco, A., Oguz, T., and Malanotte-Rizzoli, P.: Modeling dense water mass formation and winter circulation in the northern and central Adriatic Sea, Journal of Marine Systems, 20, 279-300, Doi 10.1016/S0924-7963(98)00087-6, 1999.

Bignami, F., Sciarra, R., Carniel, S., and Santoleri, R.: Variability of Adriatic Sea coastal turbid waters from SeaWiFS imagery, J Geophys Res-Oceans, 112, Artn C03s10 10.1029/2006jc003518, 2007.

Bohm, E., Banzon, V., D'Acunzo, E., D'Ortenzio, F., and Santoleri, R.: Adriatic Sea surface temperature and ocean colour variability during the MFSPP, Ann Geophys-Germany, 21, 137-149, 2003.

Boldrin, A., Langone, L., Miserocchi, S., Turchetto, M., and Acri, F.: Po River plume on the Adriatic continental shelf: Dispersion and sedimentation of dissolved and suspended matter during different river discharge rates, Mar Geol, 222, 135-158, 10.1016/j.margeo.2005.06.010, 2005.

Boldrin, A., Carniel, S., Giani, M., Marini, M., Aubry, F. B., Campanelli, A., Grilli, F., and Russo, A.: Effects of bora wind on physical and biogeochemical properties of stratified waters in the northern Adriatic, J Geophys Res-Oceans, 114, Artn C08s92 10.1029/2008jc004837, 2009.

Borzelli, G. L. E.: Scales and variability of the sea surface temperature distribution in the Adriatic Sea, J Geophys Res-Oceans, 113, Artn C11s01 10.1029/2007jc004396, 2008.

Braga, F., Giardino, C., Bassani, C., Matta, E., Candiani, G., Strombeck, N., Adamo, M., and Bresciani, M.: Assessing water quality in the northern Adriatic Sea from HICO (TM) data, Remote Sens Lett, 4, 1028-1037, 10.1080/2150704X.2013.830203, 2013.

Brando, V. E., Dekker, A. G., Park, Y. J., and Schroeder, T.: Adaptive semianalytical inversion of ocean color radiometry in optically complex waters, Applied Optics, 51, 2808-2833, 2012.

Brodie, J., Schroeder, T., Rohde, K., Faithful, J., Masters, B., Dekker, A., Brando, V., and Maughan, M.: Dispersal of suspended sediments and nutrients in the Great Barrier Reef lagoon during river-discharge events: conclusions from satellite remote sensing and concurrent flood-plume sampling, Marine and Freshwater Research, 61, 651-664, doi:10.1071/MF08030, 2010.

Castellarin, A., and Vai, G. B.: Guida alla Geologia del Sudalpino Centro-Oriental, Guide Geologiche Regionali., Soc. Geol. Ital.,, Bologna, 1982.

Chang, G. C., Dickey, T. D., Schofield, O. M., Weidemann, A. D., Boss, E., Pegau, W. S., Moline, M. A., and Glenn, S. M.: Nearshore physical processes and bio-optical properties in the New York Bight, Journal of Geophysical Research, 107, 3133, 3110.1029/2001JC001018, http://dx.doi.org/10.1029/2001JC001018, 2002.

Cozzi, S., and Giani, M.: River water and nutrient discharges in the Northern Adriatic Sea: current importance and long term changes,, Cont. Shelf Res., 31, 1881-1893, , doi:10.1016/j.csr.2011.08.010., 2011.

D'Sa, E. J., Miller, R., and McKee, B. A.: Suspended particulate matter dynamics in coastal waters from ocean color: application to the northern Gulf of Mexico, Geophys. Res. Lett. , 34, L23611, doi:10129/2007GL031192., 2007.

DeGobbis, D., Precali, R., Ivancic, I., Smodlaka, N., Fux, D., and Kveder, S.: Long-term changes in the northern Adriatic ecosystem related to anthropogenic eutrophication, , Int. J. Environ. Poll., 13,, 495-533, doi:10.1504/IJEP.2000.002332., 2000.

Devlin, M. J., and Schaeffelke, B.: Spatial extent of riverine flood plumes and exposure of marine ecosystems in the Tully coastal region, Great Barrier Reef., Marine and Freshwater Research, 60, 1109-1122, doi:10.1071/MF08343, 2009.

Dickey, T.: Emerging ocean observations for interdisciplinary data assimilation systems, Journal of Marine Systems, 40-41, 5-48, http://dx.doi.org/10.1016/S0924-7963(03)00011-3, 2003.

Dinelli, E., and Lucchini, F.: Sediment supply to the Adriatic sea basin from the Italian rivers: geochemical features and environmental constraints, Giornale Geol., 61, 121–135, 1999.

Dogliotti, A., Ruddick, K., Nechad, B., Doxaran, D., and Knaeps, E.: A single algorithm to retrieve turbidity from remotely-sensed data in all coastal and estuarine waters., Remote Sens. Environ., 156, 157-168, doi:10.1016/j.rse.2014.09.020., 2015.

Falcieri, F. M., Benetazzo, A., Sclavo, M., Russo, A., and Carniel, S.: Po River plume pattern variability investigated from model data, Cont. Shelf Res., , Cont. Shelf Res., 87, 84-95, doi:10.1016/j.csr.2013.11.001., 2014.

Falcini, F., Khan, N. S., Macelloni, L., Horton, B. P., Lutken, C. B., McKee, K. L., Santoleri, R., Colella, S., Li, C., Volpe, G., D'Emidio, M., Salusti, A., and Jerolmack, D. J.: Linking the historic 2011 Mississippi River flood to coastal wetland sedimentation, Nat. Geosci., 5, 803-807, doi:10.1038/ngeo1615., 2012.

Fisher, J. I., and Mustard, J. F.: High spatial resolution sea surface climatology from Landsat thermal infrared data, Remote Sens Environ, 90, 293-307, 10.1016/j.rse.2004.01.008, 2004.

Franz, B. A., Bailey, S. W., Kuring, N., and Werdell, P. J.: Ocean color measurements with the Operational Land Imager on Landsat-8: implementation and evaluation in SeaDAS, J. Appl. Remote Sens., 9, 096070, doi:10.1117/1.JRS.9.096070., 2015.

Gacic, M., Marullo, S., Santoleri, R., and Bergamasco, A.: Analysis of the seasonal and interannual variability of the sea surface temperature field in the Adriatic Sea from AVHRR data (1984-1992), J Geophys Res-Oceans, 102, 22937-22946, Doi 10.1029/97jc01720, 1997.

Geyer, W. R., Hill, P. S., and Kineke, G. C.: The transport, transformation and dispersal of sediment by buoyant coastal flows, Cont Shelf Res, 24, 927-949, 10.1016/j.csr.2004.02.006, 2004.

Hellweger, F. L., Schlosser, P., Lall, U., and Weissel, J. K.: Use of satellite imagery for water quality studies in New York Harbor, Estuarine, Coastal and Shelf Science, 61, 437-448, 2004.

Hestir, E. L., Brando, V. E., Bresciani, M., Giardino, C., Matta, E., Villa, P., and Dekker, A. G.: Measuring freshwater aquatic ecosystems: The need for a hyperspectral global mapping satellite mission, Remote Sens. Environ, 167 181-195, doi:10.1016/j.rse.2015.05.023., 2015.

Hetland, R. D.: Relating River Plume Structure to Vertical Mixing,, J. Phys. Oceanogr.,, 35, 1667-1688, , doi:10.1175/JPO2774.1, 2005.

Hickey, B. M., Geier, S. L., Kachel, N. B., and MacFadyen, A.: A bi-directional river plume: The Columbia in summer, Cont. Shelf Res., 25, 1631-1656, doi:10.1016/j.csr.2005.04.010., 2005.

Horner-Devine, A. R., Hetland, R. D., and MacDonald, D. G.: Mixing and Transport in Coastal River Plumes, Annu. Rev. Fluid Mech, 47, 569-594, doi:10.1146/annurev-fluid-010313-141408, 2015.

Irons, J. R., Dwyer, J. L., and Barsi, J. A.: The next Landsat satellite: The Landsat Data Continuity Mission, Remote Sens. Environ., 122, 11-21, doi:10.1016/j.rse.2011.08.026, 2012.

Janssen, P. A. E. M., Abdalla, S., Hersbach, H., and Bidlot, J. R.: Error estimation of buoy, satellite, and model wave height data, , J. Atmos. Ocean. Tech., 24, 1665-1677,, doi:10.1175/JTECH2069.1., 2007.

Margvelashvili, N., Andrewartha, J., Herzfeld, M., Robson, B., and Brando, V. E.: Satellite data assimilation and estimation of a 3d coastal sediment transport model using error-subspace emulators, Environmental Modelling & Software, 40, 191–201, 10.1016/j.envsoft.2012.09.009,, 2013.

Marini, M., Jones, B. H., Campanelli, A., Grilli, F., and Lee, C. M.: Seasonal variability and Po River plume influence on biochemical properties along western Adriatic coast, J. Geophys. Res-Oceans, 113, C05S90, doi:10.1029/2007JC004370., 2008.

Melin, F., Vantrepotte, V., Clerici, M., D'Alimonte, D., Zibordi, G., Berthon, J.-F., and Canuti, E.: Multi-sensor satellite time series of optical properties and chlorophyll-a

concentration in the Adriatic Sea, Progress in Oceanography, 9, 229–244, doi:10.1016/j.pocean.2010.12.001, 2011.

Montanari, A.: Hydrology of the Po River: looking for changing patterns in river discharge, Hydrol. Earth Syst. Sci, 16, 3739-3747, doi:10.5194/hess-16-3739-2012., 2012.

Mouw, C. B., Greb, S., Aurin, D., DiGiacomo, P. M., Z. Lee, Twardowski, M., Binding, C., C. Hu, Ma, R., Moore, T., Moses, W., and Craig, S. E.: Aquatic color radiometry remote sensing of coastal and inland waters: Challenges and recommendations for future satellite missions, Remote Sens. Environ., 160, 15-30, doi:10.1016/j.rse.2015.02.001, 2015.

Nof, D., and Pichevin, T.: The ballooning of outflows, J Phys Oceanogr, 31, 3045-3058, Doi 10.1175/1520-0485(2001)031<3045:Tboo>2.0.Co;2, 2001.

Otero, P., Ruiz-Villarreal, M., and Peliz, Á.: Variability of river plumes off North- west Iberia in response to wind events, J. Mar. Syst., 72, 238-255, doi:10.1016/j.jmarsys.2007.05.016., 2008.

Otero, P., Ruiz-Villarreal, M., and Peliz, Á.: River plume fronts off NW Iberia from satellite observations and model data., J. of Mar. Sci, 66, 1853-1864, doi:10.1093/icesjms/fsp156., 2009.

Pahlevan, N., Lee, Z., Wei, J., Schaaf, C. B., Schott, J. R., and Berk, A.: On-orbit radiometric characterization of OLI (Landsat-8) for applications in aquatic remote sensing, Remote Sens. Environ.,, 154, 272-284, doi:10.1016/j.rse.2014.08.001, 2014.

Palacios, S. L., Peterson, T. D., and Kudela, R. M.: Development of synthetic salinity from remote sensing for the Columbia River plume, J. Geophys. Res., doi:10.1029/2008JC004895., 2009.

Pietrzak, J. D., Boer, G. J. d., and Eleveld, M. A.: Mechanisms controlling the intra-annual mesoscale variability of SST and SPM in the southern North Sea, Cont. Shelf Res., 31, 594-610, doi:10.1016/j.csr.2010.12.014., 2011.

Pigorini, B.: Sources and dispersion of recent sediments of the Adriatic Sea, , Mar. Geol., 3, 187-229, doi:10.1016/0025-3227(68)90031-5., 1968.

Piovan, S., Mozzi, P., and Stefani, C.: Bronze Age paleohydrography of the southern Venetian Plain, Geoarchaeology, 25, 6-35, doi:10.1002/gea.20300., 2010.

Raicich, F.: Note on the flowrates of the Adriatic rivers. Tech. Rep. RF 02/94, CNR Istituto Sperimentale Talassografico, Trieste, Italy, 8, 1994.

Robinson, I. S.: Discovering the Ocean from Space The Unique Applications of Satellite Oceanography Springer, Heidelberg, 638 pp., 2010.

Russo, A., Carniel, S., and Benetazzo, A.: Support for ICZM and MSP in the Adriatic Sea region., Sea Technol., 54, 27-35, 2013a.

Russo, A., Coluccelli, A., Carniel, S., Benetazzo, A., Valentini, A., Paccagnella, T., Ravaioli, M., and Bortoluzzi, G.: Operational models hierarchy for short term marine predictions: the Adriatic Sea example, MTS/IEEE OCEANS, Bergen, 2013b.

Schroeder, T., Devlin, M. J., Brando, V. E., Dekker, A. G., Brodie, J. E., Clementson, L. A., and McKinna, L.: Inter-annual variability of wet season freshwater plume extent into the Great Barrier Reef lagoon based on satellite coastal ocean colour observations, Marine Pollution Bulletin, 65, 210-223, 10.1016/j.marpolbul.2012.02.022, 2012.

Sclavo, M., Benetazzo, A., Carniel, S., Bergamasco, A., Falcier, F. M., and Bonaldo, D.: Wave-current interaction effect on sediment dispersal in a shallow semi-enclosed basin, J Coastal Res, 1587-1592, 10.2112/SI65-268.1, 2013.

Simpson, J. H.: Physical processes in the ROFI regime, J. Mar. Syst., 12, 3-15, 10.1016/S0924-7963(96)00085-1, 1997.

Solidoro, C., Bastianini, M., Bandelj, V., Codermatz, R., Cossarini, G., Canu, D. M., Ravagnan, E., Salon, S., and Trevisani, S.: Current state, scales of variability, and trends of biogeochemical properties in the northern Adriatic Sea, J. Geophys. Res-Oceans, 114, C07S91, 10.1029/2008JC004838, 2009.

Spillman, C. M., Imberger, J., Hamilton, D. P., Hipsey, M. R., and Romero, J. R.: Modelling the effects of Po River discharge, internal nutrient cycling and hydrodynamics on biogeochemistry of the northern Adriatic Sea, J. Mar. Syst., 68, 167-200, 10.1016/j.jmarsys.2006.11.006, 2007.

Stanev, E. V., Schulz-Stellenfleth, J., Staneva, J., Grayek, S., Seemann, J., and Petersen, W.: Coastal observing and forecasting system for the German bight-estimates of hydrophysical states, Ocean Sci., 7, 569-583, 10.5194/os-7-569-2011, 2011.

Staneva, J., Stanev, E. V., Wolff, J.-O., Badewien, T. H., Reuter, R., Flemming, B., Bartholoma, A., and Bolding, K.: Hydrodynamics and sediment dynamics in the German Bight. A focus on observations and numerical modeling in the East Frisian Wadden Sea, Cont. Shelf Res., 29, 302-319, 10.1016/j.csr.2008.01.006, 2009.

Storey, J., Choate, M., and Moe, D.: Landsat 8 Thermal Infrared Sensor Geometric Characterization and Calibration, Remote Sens-Basel, 6, 11153-11181, 10.3390/rs61111153, 2014.

Syvitski, J. P., Kettner, A. J., Correggiari, A., and Nelson, B. W.: Distributary channels and their impact on sediment dispersal, Mar. Geol., 222, 75-94, 10.1016/j.margeo.2005.06.030, 2005.

Tesi, T., Miserocchi, S., Goni, M. A., Turchetto, M., Langone, L., De Lazzari, A., Albertazzi, S., and Correggiari, A.: Influence of distributary channels on sediment and organic matter supply in event-dominated coastal margins: the Po prodelta as a study case, Biogeosciences, 8, 365-385, 10.5194/bg-8-365-2011, 2011.

Ullman, D. S., and Cornillon, P. C.: Satellite-derived sea surface temperature fronts on the continental shelf off the northeast US coast, J. Geophys. Res., 104C, 23459-23478, 10.1029/1999JC900133, 1999.

Vanhellemont, Q., and Ruddick, K.: Turbid wakes associated with offshore wind turbines observed with Landsat 8, Remote Sens. Environ., 145, 105-115, 10.1016/j.rse.2014.01.009, 2014.

Vanhellemont, Q., and Ruddick, K.: Advantages of high quality SWIR bands for ocean colour processing: Examples from Landsat-8, Remote Sens. Environ, 161, 89-106, 10.1016/j.rse.2015.02.007, 2015.

Vantrepotte, V., Loisel, H., Dessailly, D., and Mériaux, X.: Optical classification of contrasted coastal waters, Remote Sens. Environ., 123, 306-323, 10.1016/j.rse.2012.03.004, 2012.

Warner, J. C., Sherwood, C. R., Signell, R. P., Harris, C., and Arango, H. G.: Development of a three-dimensional, regional, coupled wave, current, and sediment-transport model, Comput. Geosci., 34, 1284-1306, 10.1016/j.cageo.2008.02.012, 2008.

Zasso, M., and Settin, T.: Sulla ripartizione delle portate del Po tra i vari rami e le bocche a mare del delta: esperienze storiche e nuove indagini all'anno 2011 (in Italian). Relazione n. 02/12, ARPAV Dipartimento Regionale Per La Sicurezza Del Territorio, Belluno, Italy, 47, 2012.

Zavatarelli, M., Raicich, F., Bregant, D., A. Russo, and Artegiani, A.: Climatological biogeochemical characteristics of the Adriatic Sea, , J. Mar. Syst., 18, 227-263, 10.1016/S0924-7963(98)00014-1, 1998.
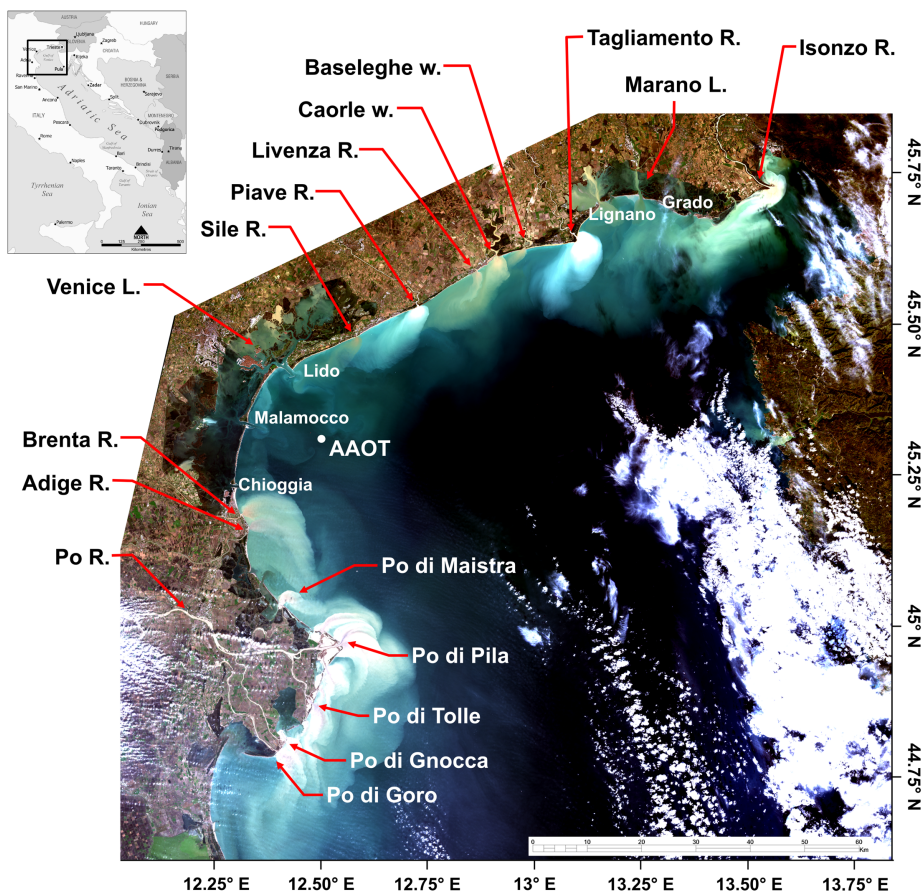
Figure 1. Study site with the location of rivers (R.), lagoons (L.) and wetlands (w.). Pseudo true colour Landsat-8 OLI imagery acquired on 19 November 2014.
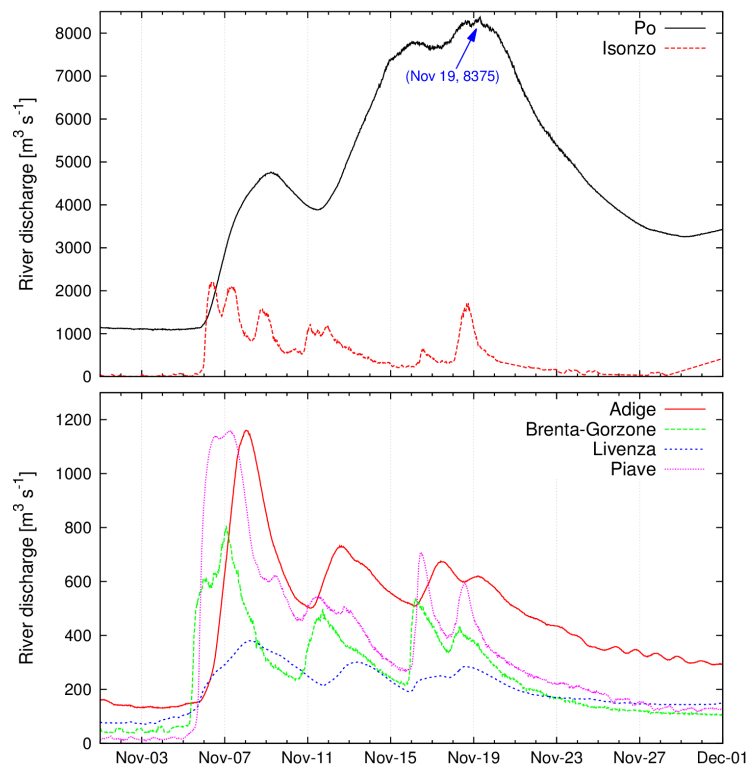
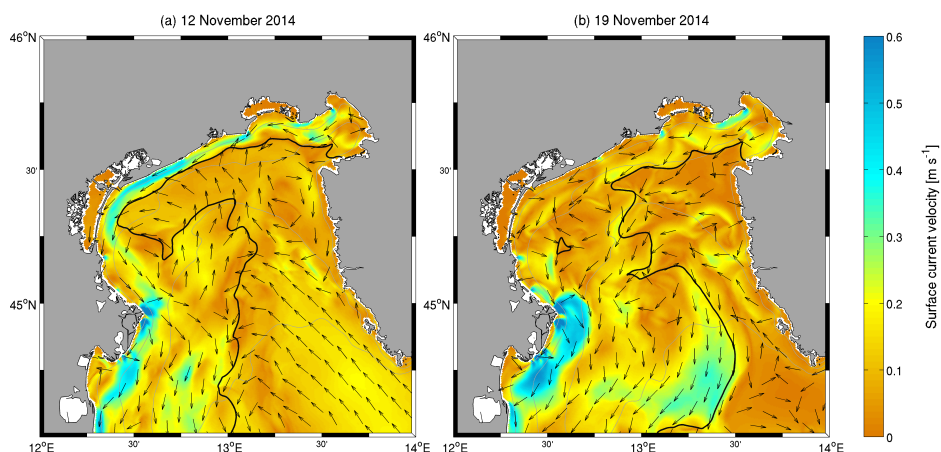Figure 2. River discharge for November 2014 for the main rivers flowing in NAS.

Figure 3. Daily-averaged modelled surface currents velocities in the NAS on 12 November 2014 (a) and 19 November 2014 (b). Normalized vectors indicating current direction have been subsampled every 15 grid points for graphical purposes, black thick line indicates modelled isohaline 36.
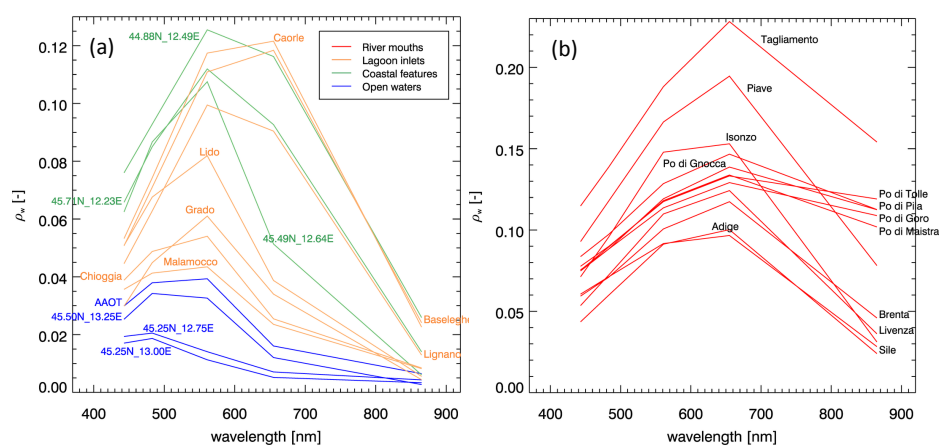
Figure 4. Reflectance spectra extracted from selected locations in NAS, including open waters, coastal features, lagoon inlets (a), and river mouths (b).
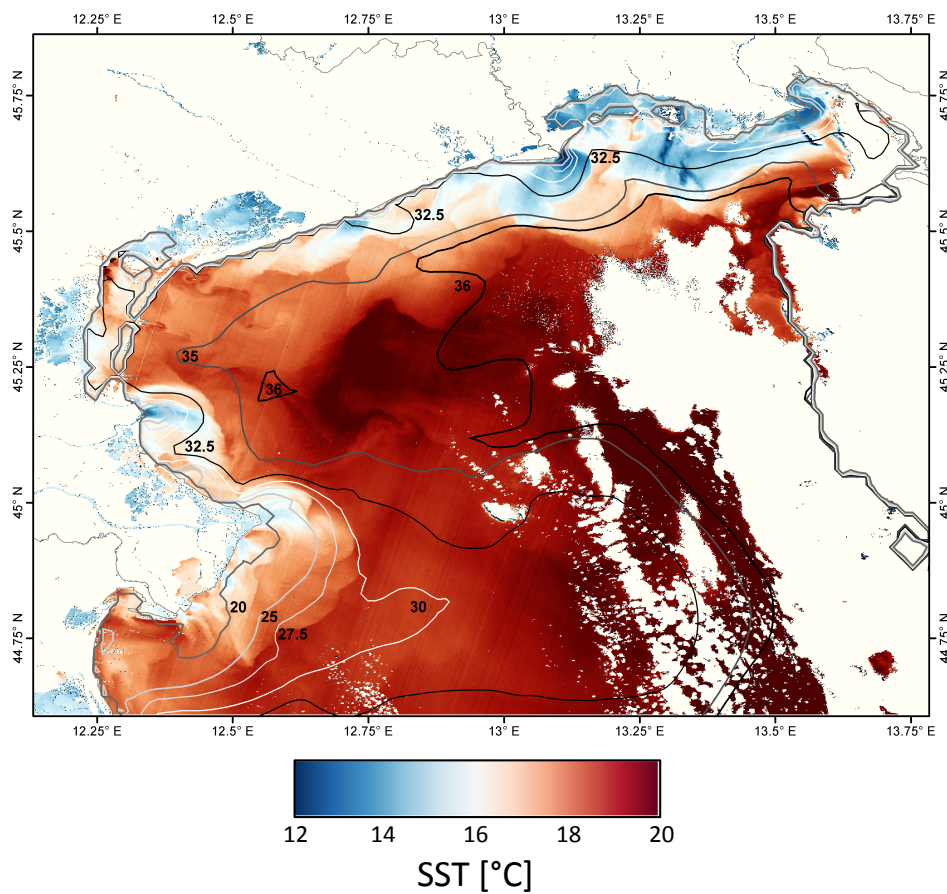
Figure 5. SST field estimated from Landsat-8 TIRS imagery acquired on 19 November 2014. Isohalines from the modelled SSS field are overlaid.
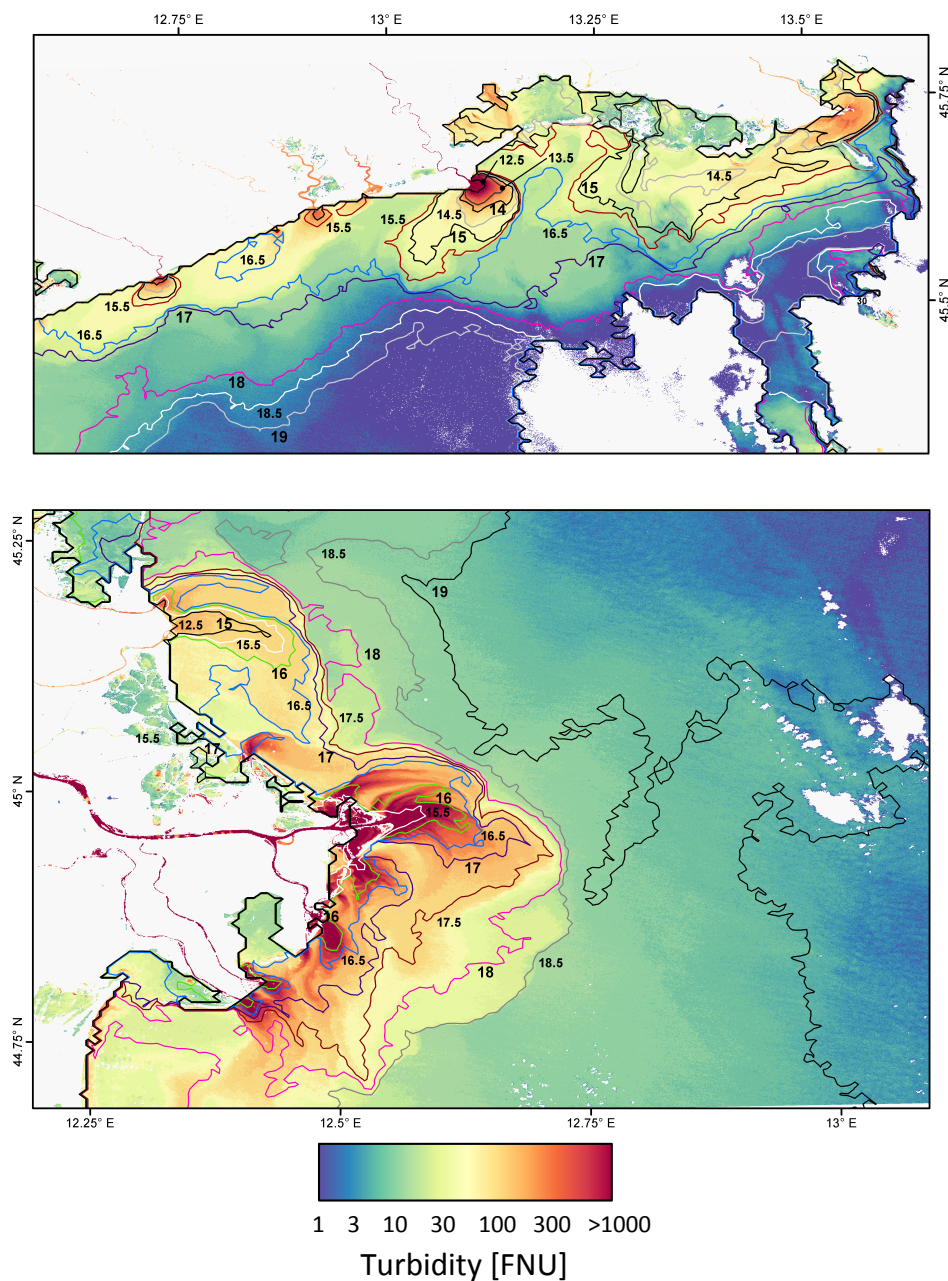
Figure 6. Turbidity map estimated from Landsat-8 OLI imagery acquired on 19 November 2014: a) all the plumes from the Isonzo to the Piave River, b) the Brenta, Adige and Po river plumes. Isotherms from the Landsat-8 TIRS SST field are overlaid. To enhance readability some isotherms have different colour coding in the two areas.
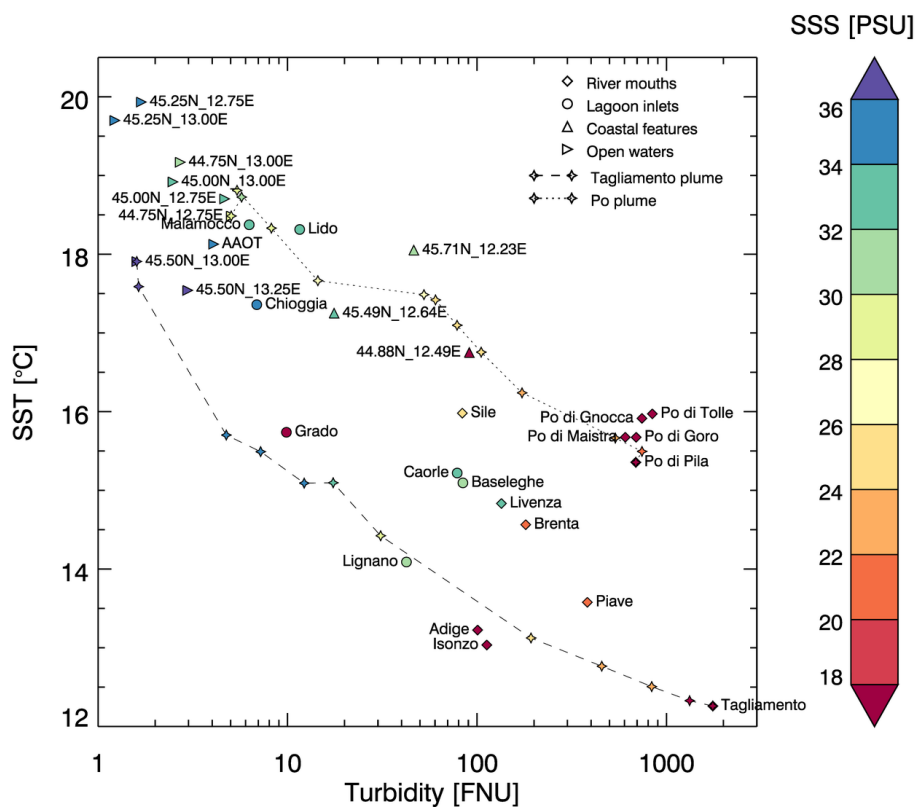
Figure 7 Relations between Turbidity, SST and SSS for selected locations in NAS. The dilution of the Po and Tagliamento river plumes across the SSS gradient is shown with dashed lines.